U.PORTO

MESTRADO INTEGRADO EM MEDICINA

Clinical Applications of Amide Proton Transfer (APT) in the Evaluation of Cerebral Astrocytomas

Maria Gabriela Pinto de Sá Almeida

M

2024

Clinical Applications of the Amide Proton Transfer (APT) Technique in the Evaluation of Cerebral Astrocytomas

Projeto de Investigação

Dissertação de candidatura ao grau de Mestre em Medicina, submetida ao Instituto de Ciências Biomédicas Abel Salazar - Universidade do Porto.

Estudante: Maria Gabriela Pinto de Sá Almeida
Mestrado Integrado em Medicina
Instituto de Ciências Biomédicas Abel Salazar - Universidade do Porto
Número institucional: 201807744
Endereço de e-mail: up201807744@edu.icbas.up.pt

Orientador: Dr. João Xavier
Assistente Graduado Sénior - Serviço de Neurorradiologia ULS Santo António
Professor Catedrático Convidado - Instituto de Ciências Biomédicas Abel Salazar - Universidade do Porto

Coorientador: Prof. Doutor Ricardo Taipa
Assistente Hospitalar Graduado – Serviço de Neuropatologia ULS Santo António
Professor Associado Convidado – Instituto de Ciências Biomédicas Abel Salazar – Universidade do Porto

MAIO 2024

Declaração de Integridade Científica

Este estudo foi autorizado pela Comissão de Ética da ULSSA|ICBAS, pela Direção do Centro Académico Clínico ICBAS-CHP e pelo Presidente do Conselho de Administração e pelo Conselho de Administração da ULSSA.

Ref.ª: 2023.264(226-DEFI/216-CE)

Acknowledgements

First and foremost, I must thank Dr João Xavier MD, for receiving me kindly, for his scientific knowledge and willingness to tech, and for his time and dedication to this project. I would also like to thank my co-advisor, Professor Ricardo Taipa MD, PhD, for his valuable and pertinent input.

I would also like to show my gratitude towards everyone in the Neuroradiology department at ULS Santo António, for their help and guidance, especially Dr Cristina Ramos MD, for her guidance and support whenever I was in need, and also Dr Catarina Pinto MD, and Dr Liliana Igreja MD, for their support in the practical stages of this project.

Despite not having a direct involvement, I must thank my family and friends for their support.

Resumo

Contexto: Os astrocitomas são um grupo heterogéneo de tumores primários do sistema nervoso central (SNC) com elevado potencial infiltrativo e elevada mortalidade. Consistem tipicamente num núcleo de tumor sólido com áreas de necrose, rodeado por edema, que pode, ou não, estar infiltrado por células malignas. Embora a ressonância magnética (RM) seja o método atual para a avaliação não invasiva (pré-cirúrgica) destes tumores, apresenta algumas limitações, por exemplo, relacionadas com a sua capacidade limitada de estadiamento e delimitação das margens tumorais.

Durante a cirurgia de resseção tumoral, tenta-se limitar a remoção do tecido cerebral edemaciado, pois corresponde a áreas que podem, eventualmente, vir a recuperar a sua função normal após o tratamento cirúrgico. Consequentemente, há uma necessidade urgente de uma nova técnica de imagem que seja capaz de fazer uma distinção mais precisa entre o tecido cerebral potencialmente recuperável e aquele que deve ser removido. O Amide-Proton Transfer (APT) é uma nova técnica de RM que pode fornecer informações visuais e quantitativas mais precisas sobre o grau e as margens tumorais, distintas daquelas fornecidas pelas sequências convencionais de RM atualmente em uso.

Objetivos: O objetivo deste estudo é avaliar as aplicações clínicas do APT num ambiente de rotina clínica, para a avaliação inicial de astrocitomas no cérebro humano, focando-nos na sua capacidade de distinção entre tumor e edema peritumoral e na correlação entre a intensidade do sinal e o grau histopatológico do tumor.

Materiais e Métodos: Nove pacientes com achados imagiológicos sugestivos de glioma, e nos quais previámos que o APT fosse fornecer informações adicionais foram selecionados. A sequência de APT foi adicionada ao protocolo básico de aquisição de imagens, e todas as imagens foram analisadas. Os valores de intensidade do sinal APT foram obtidos desenhando regiões de interesse (ROIs) nas áreas correspondentes ao núcleo do tumor, periferia do tumor e substância branca contralateral de aparência normal (CNAWM). Foi feito um estudo comparativo entre as imagens APT e as respetivas medições, as sequências convencionais de ressonância e os achados histopatológicos para cada tumor.

Resultados: Foram estudados dois tumores de grau 4, dois tumores de grau 3, três tumores de grau 2 e dois tumores sem diagnóstico definitivo (com achados imagiológicos na ressonância sugestivos de lesões de baixo grau). Para tumores de alto grau, a intensidade do sinal APT medida foi significativamente maior no tumor do que na substância branca contralateral de aparência normal

(CNAWM). Para além disso, em tumores de alto grau captantes, a intensidade no *core* tumoral foi significativamente maior em comparação com a intensidade nas regiões consideradas periferia do tumor, e com a CNAWM. Para tumores de baixo grau, a intensidade do APT foi também significativamente maior na região do tumor em comparação com a CNAWM, mas esse aumento não foi tão significativo como nos tumores de alto grau. Por fim, ao comparar as intensidades de sinal obtidas em tumores de alto e baixo grau, os tumores de alto grau apresentaram um aumento significativamente maior em comparação com os tumores de baixo grau.

Conclusões: As imagens de APT foram capazes de fornecer novos dados para caracterização dos tumores estudados, potencialmente delimitando o núcleo do tumor do edema peritumoral acrescentando precisão às técnicas de contraste usadas atualmente, revelando-se uma ferramenta potencialmente útil para o planeamento do tratamento cirúrgico. Também foi encontrada uma correlação entre a intensidade do sinal APT e o grau histopatológico do tumor, permitindo distinguir tumores cerebrais de alto e baixo grau com mais precisão do que as sequências de RM atualmente em uso. Para além disso, esta técnica foi capaz de identificar áreas de maior agressividade dentro de um tumor, um achado significativo, visto que permite decidir o local mais indicado para realizar a biópsia e determinar corretamente o grau histopatológico do tumor.

Abstract

Context: Astrocytomas are a heterogenous group of primary central nervous system (CNS) tumors with a high infiltrative potential and elevated mortality rate. They typically consist of a solid tumor core with areas of necrosis, surrounded by regions of edema, which may or may not be infiltrated with malignant cells. Although magnetic resonance imaging (MRI) is the method currently in use for a non-invasive (pre-surgical) evaluation of brain tumors, it still has several limitations, for example, related to its limited capacity for grading and delineating tumor boundaries.

Tumoral resection surgery attempts to limit the resection of edematous brain tissue, as these areas may be able to recover normal function after surgical treatment. Consequently, there is an urgent need for a new imaging technique, that can make a more accurate distinction between potentially recoverable brain tissue, and the one that needs to be removed. Amide-Proton Transfer (APT) imaging is a new MRI technique that may provide more accurate visual and quantitative information about tumor grade and margins, distinct from that provided by conventional MRI sequences currently in use.

Aim of the study: The aim of this study is to assess the clinical applications of APT-weighted (APT-w) imaging in a clinical routine setting in the initial evaluation of astrocytomas in the human brain, focusing on its ability to distinguish tumor from peritumoral edema, and seeking a correlation between APT signal intensity and the histopathologic grade of a tumor.

Materials and Methods: Nine patients with brain lesions whose MRI findings suggested the diagnosis of glioma, and in whom we predicted APT-w imaging would be able to provide additional information were selected. APT-w imaging sequence was added to the basic image acquisition protocol and all images were analyzed. Values for APT signal intensity were obtained by drawing regions of interest (ROIs) in areas corresponding to tumor core, tumor periphery, and contralateral normal appearing white matter (CNAWM). A comparative analysis between APT-weighted sequences and their respective APT signal intensity measurements, conventional MR sequences and histopathological findings for each tumor was performed.

Results: Two WHO Grade 4, two WHO Grade 3, three WHO Grade 2, and two tumors without a final diagnosis were studied. For high-grade tumors, APT signal intensity was found to be significantly higher in the tumor region than in the CNAWM. Furthermore, in high-grade tumors with gadolinium enhancement, the tumor core intensity was found to be much higher in comparison to the intensity in regions assumed to represent tumor periphery, and also to the CNAWM. For low-grade tumors,

APT intensity was also found to be significantly higher in the tumor region in comparison to the CNAWM, but this increase was not as significant as for high-grade tumors. Finally, when comparing signal intensities obtained in tumors of high and low-grade, high-grade tumors appeared to have a significant increase in signal in comparison to low-grade tumors.

Conclusion: APT images were able to provide new data for the characterization of tumors, potentially delineating tumor core from peritumoral edema more accurately than gadolinium-based imaging alone, revealing a potentially useful tool when planning surgical treatment. APT signal intensity has also been found to be correlated to histopathologic grade, allowing it to distinguish high from low-grade tumors with more accuracy than conventional MR images alone. Moreover, this technique was also able to identify areas of higher malignancy within a tumor, which is a significant finding, as it allows for the choice of the most appropriate location to biopsy and a more accurate determination of the histopathological grade of a tumor.

Key Words: CEST; APT; magnetization transfer; brain tumor; astrocytoma; MRI.

List of Acronyms

APT: Amide-Proton Transfer

APT-w: Amide-Proton Transfer weighted

CEST: Chemical Exchange Saturation Transfer

CNAWM: Contralateral Normal Appearing White Matter

CNS: Central Nervous System

FLAIR: Fluid Attenuated Inversion Recovery

f-MRI: Functional Magnetic Resonance Imaging

Gd-T1w: Gadolinium T1-weighted

LGA: Low-grade Astrocytoma

LGO: Low-grade Oligodendroglioma

MR: Magnetic Resonance

MRI: MR Imaging

MRSI: MR Spectroscopic Imaging

NAWM: Normal appearing white matter

PET: Positron Emission Tomography

rCBV: Relative Cerebral Blood Volume

RF: Radiofrequency

ROI: Region of interest

T1-w: T1-weighted

T2-w: T2-weighted

ULSSA: *Unidade Local de Saúde - Santo António*

WHO: World Health Organization

Index

Introduction

In brain tumor resection surgery, the extent of resection is positively correlated with survival. However, due to its diffuse and invasive nature, the identification of malignant tissue is extremely difficult, making tumor resection surgery and its pre-operative planning imaging guided. During tumor resection, the goal is to find balance between maximizing the extent of resection and preserving brain functions since surgery-induced neurological deficits result in a lower quality of life and shortened survival.[1]

The current standard imaging techniques used in daily clinical practice for the evaluation of brain tumors are T2-weighted (T2-w), T2 Fluid Attenuated Inversion Recovery (T2-FLAIR) and T1-weighted (T1-w) images, with and without gadolinium enhancement.[1,2] Other imaging modalities, such as positron emission tomography (PET), and intraoperative techniques, including the use of fluorescence, are also available. More recently, function-oriented sequences have been introduced such as perfusion[3,4] and diffusion studies,[5,6,7] and proton magnetic resonance spectroscopy imaging (MRSI).[8,9,10] The localization of important brain functions and white matter tracts is possible with functional magnetic resonance imaging (f-MRI), diffusion tensor imaging, magnetoencephalography, and navigated transcranial magnetic stimulation.[1] These techniques are used for localizing, diagnosing and characterizing brain tumors as well as to guide treatments and assess its effects.[11]

Nevertheless, although MRI is the standard of care for assessing brain tumors before, during, and after treatment, these imaging techniques sill have several limitations, especially regarding its ability to determine tumor grade or to separate solid tumor from peritumoral edema. When it comes to delineating tumor boundaries, for example, the hyperintensity observed on a T2-w image of a glial brain tumor may be either due to tumor infiltration or peritumoral vasogenic edema.[12,13,14] At the same time, a Gadolinium-T1w (Gd-T1w) image only reveals focal areas of malignant tissue if the blood-brain barrier is disrupted.[15] These limitations pose a challenge for the accurate planning of surgical treatment and for the precise resection of a brain tumor, as the imaging techniques that are currently available are unable to precisely differentiate tumor infiltration from the surrounding brain tissue.[16] MRSI may accomplish such tissue delineation, but it suffers from reduced sensitivity, limited spatial resolution and increased scanning time.[8,9,10]

Chemical exchange saturation transfer (CEST) imaging is a recent molecular imaging technique which works as a new contrast mechanism for MRI.[17,18,19] It uses selective radiofrequency (RF) saturation of specific protons whose magnetization is then transferred via chemical exchange and

dipolar interactions, to protons in bulk water, lowering its signal.[19-24] The degree of signal suppression is greater for tissues with high protein content and high rates of water-macromolecular interactions.[22,24-29] Currently, the most widely used type of CEST imaging is amide proton transfer (APT) imaging which generates contrast based on the saturation of amide protons in the peptide bonds of mobile proteins and peptides.[13, 29-35] When a selective RF pulse is applied at 3.5 ppm downfield from the water resonance, the protons attached to the amide bond become saturated, subsequently moving to the neighboring water and are exchanged with the free water protons. APT values in tissues typically range between -5 and 5% and can be displayed as color maps overlaid on conventional images.[22,24-29] APT-weighted (APT-w) MRI has been used in several applications to evaluate brain tumors, showing potential as a tool for brain tumor detection, grading, identification of genetic markers and treatment monitoring. It may also potentially aid in guiding brain tumor treatments, such as surgery, radiotherapy and local chemotherapy.[11]

The reason for the increase in APT signal found in high-grade brain tumors in comparison to peritumoral edema and contralateral normal-appearing white matter (CNAWM), is the fact that they are highly cellular tissues, where many proteins are over-expressed.[36] The hyperintense regions usually appear larger than the areas of contrast enhancement on Gd-T1w images, but smaller than the areas identified as tumor on T2-w, T1-w and FLAIR, due to its potential ability to delineate tumor boundaries, superior to that of morphological sequences currently used. This ability means that APT-w imaging has the potential to become extremely helpful in planning maximal tumor resection, which is especially important as about 80% of recurring brain tumors occur at the resection margin.[37-43]

Besides being able to differentiate solid tumor from peritumoral edema, and accurately define tumor boundaries, APT signal has also been found to offer additional information related to the histopathologic grade of gliomas. Currently, perfusion studies are considered the best method of estimating histopathologic grade, by using the relative cerebral blood volume (rCBV). High-grade gliomas (World Health Organization [WHO] grades 3 and 4) have regions of higher rCBV in comparison to low-grade gliomas (WHO grades 1 and 2). Exceptions to this rule include the pilocytic astrocytoma and oligodendroglioma, which can show foci of high rCBV that does not relate to tumor grade.[44] In turn, APT-w hyperintensity is associated with high-grade gliomas, while APT-w isointensity was observed predominantly in low-grade gliomas.[45-53] This happens due to the fact that APT-w imaging indirectly reflects protein content and high-grade tumors tend to show accelerated cell proliferation and increased protein expression in comparison to low-grade tumors. A recent study has shown that APT-w imaging has a linear positive correlation with the

pathologic tissue proliferative index and cell density.[54] This is an important advantage of APT-w imaging, as gadolinium-enhancement in MRI is not always specific for tumor grading (low grade gliomas occasionally enhance[55] and some high-grade gliomas show no enhancement[56]). Furthermore, APT-w imaging can identify high-grade regions within heterogeneous gliomas, allowing for more precise biopsies of the most aggressive region of a tumor[45-53]. This technique has the potential to become a valuable imaging biomarker for distinguishing high from low-grade gliomas and detecting high-grade tumors with no gadolinium enhancement as well as enhancing low-grade gliomas.[11]

Another, more recent use for this technique is to distinguish active glioma from normal treatment effects.[57] When assessing radiation treatment, tumors appear to enlarge during the first several weeks (12 weeks) as judged from T2-w and gadolinium-enhancement MRI. Meanwhile APT-w signal gradually decreases, appearing hypo or isointense compared to normal-appearing contralateral tissue.[58] This happens because, in post-treatment imaging, enhancement can result from other causes, besides tumoral growth.[59] Radiation necrosis, for example, is associated with the absence of mobile cytosolic proteins due to the loss of cytoplasm and organelles, thus appearing as hypointense or isointense in an APT-w MRI.[11] Several studies have shown that APTw imaging provides a unique imaging method for evaluation of tumor response to radiotherapy,[59,60,61] chemotherapy[62] and high-intensity focused ultrasound therapy.[63]

Since 2003, APT-w imaging has been the subject of many scientific papers, which collect data from an investigational point of view. On the other hand, APT-w imaging is available at *Unidade Local de Saúde Santo António* (ULSSA) since September 2023 on a Phillips 3T MRI scanner installed at CMIN (Centro Materno-Infantil do Norte), but a few months after the installation, this technique had not yet been implemented into daily clinical practice.

Research Objectives:

In this study, we aim to test the feasibility of APTw imaging in a clinical routine setting and to assess its clinical applications in the initial evaluation of astrocytomas in the human brain, focusing on its ability to distinguish tumor from peritumoral edema, and how APT signal correlates to histopathological grade.

Materials and Methods

Patients with brain lesions whose MRI findings suggested the diagnosis of glioma and in whom we predicted APT-w imaging would be able to provide additional information were selected. APT-w imaging sequence was added to the basic image acquisition protocol and all images were analyzed. Four patients had already undergone surgery when these MRI images were acquired, and three of them underwent surgery afterwards. Two of the patients have not yet been operated, and so, their final diagnosis remains unknown.

The MR scanner Phillips Ingenia 3T (Software Release 5.7) was used to acquire the basic image acquisition protocol for expansive brain lesions which included: Axial T1-w (TR 663, TE 10, slice thickness 3mm, slice gap 4mm), axial 2D Gd-T1w (TR 698, TE 10, slice thickness 3mm, slice gap 4mm), 3D Gd-T1w (TR 600, TE 26.8, slice thickness 1.1mm, slice gap 0.55), axial T2-w (TR 3877, TE102, slice thickness 3mm, slice gap 3.3mm), coronal T2-w (TR 4577, TE 109, slice thickness 3mm, slice gap 3.3mm), 3D FLAIR (TR 4800, TE 340, TI 1650, slice thickness 2mm, slice gap 2mm), axial T2*-weighted images (TR 1284, TE 16, flip angle 25, slice thickness 3mm, slice gap 4mm), T2* weighted perfusion MR (TR 994, TE 40) and diffusion study (TR 5130, TE 91.5, B-value 1000, slice thickness 3mm, slice gap 4mm).

APT-w images were acquired for the nine patients. A 3D-TSE multi-point mDiXON sequence was used for amide proton saturation, which provides two series of images that allow the calculation of water amide saturation differences/asymmetry as a percentage (MTR - Magnetization Transfer Ratio) on a scale from -5% to 5%. The two series are then processed using the "Image View/Color LUT - APT-w/capture slices" application, which generates a color map.

Values for APT signal intensity were obtained by drawing regions of interest (ROIs), obtaining the mean value ± standard deviation. For gadolinium enhancing brain tumors, three ROIs were drawn, tumor core, tumor periphery, and contralateral normal-appearing white matter (CNAWM), according to the T2-FLAIR and Gd-T1w images. We assigned the whole area with T2-FLAIR abnormality as tumor, and gadolinium enhanced regions as tumor core while the non-enhancing regions were assigned as tumor periphery. For non-enhancing brain tumors, only two ROIs were drawn, tumor (region of T2-FLAIR abnormality) and CNAWM.

The statistical analysis involved measures of descriptive statistics (means and respective standard deviations) and inferential statistics. For the latter, the Student's t-test for paired samples and the Student's t-test for independent samples were used. The significance level for rejecting the null

hypothesis was set at (α) ≤ 0.05. The statistical analysis was performed using SPSS (Statistical Package for the Social Sciences) version 28 for Windows.

Results

The lesion location, post-operative or assumed diagnosis and a quantitative analysis of the APT-w images from all nine patients are shown in Table I.

Table I. APT results for human brain tumor patients.

Patient No.	Sex	Lesion Location	Previous Surgical Intervention	Diagnosis	Gadolinium Enhancement	APTw intensity (%)[a]		
						Tumor Core[b]	Tumor Periphery[c]	CNAWM
1	M	Left Temporal	No	Glioblastoma IDH-wildtype (WHO Grade 4)	Yes	2.69 ± 0.23	0.97 ± 0.2	0.86 ± 0.31
2	F	Right Frontal	Yes	Glioblastoma IDH-wildtype (WHO Grade 4)	Yes	3.36 ± 0.53	1.15 ± 0.31	0.51 ± 0.20
3	M	Left Frontotemporal	No	Astrocytoma IDH-mutated (WHO Grade 3)	No	2.21 ± 0.13[d]		0.34 ± 0.22
4	M	Left Frontoparietal	Yes	Astrocytoma IDH-mutated (WHO Grade 3)	No	1.67 ± 0.24[d]		0.35 ± 0.29
5	M	Left Parietooccipital	No	Presumed Low Grade*	No	1.29 ± 0.21[d]		0.18 ± 0.18
6	F	Right Temporal	No	Presumed Low Grade*	No	1.97 ± 0.48[d]		0.41 ± 0.24
7	F	Left Frontal	Yes	Astrocytoma IDH-mutated (WHO Grade 2)	No	0.93 ± 0.18[d]		0.61 ± 0.12
8	F	Left Frontal	Yes	Astrocytoma IDH-mutated (WHO Grade 2)	No	1.52 ± 0.4[d]		0.65 ± 0.40
9	F	Left Frontal	Yes	Oligodendroglioma IDH-mutated and 1p/19q-codeleted (WHO Grade 2)	No	1.04 ± 0.14[d]		0.87 ± 0.27

[a]Values are mean +/- SD.

[b]Identified by Gd-T1w imaging (Gd-enhancing area).

[c]Difference between areas with FLAIR abnormality and Gd-enhancement.

[d]Areas of FLAIR abnormality.

*Presumed diagnosis according to MRI findings (patients have not undergone a biopsy of the lesion).

Two patients were diagnosed with glioblastoma IDH-wildtype (WHO grade 4), two with IDH-mutated astrocytoma (WHO grade 3), and three with low-grade brain tumors (low-grade astrocytoma [LGA] or low-grade oligodendroglioma [LGO]). Two out of the nine patients selected have not yet undergone a brain biopsy, and consequently, their final diagnosis remains unknown.

For high-grade tumors (N = 4), APT image intensity was found to be significantly higher in the tumor region than in the CNAWM ($p = 0.009$, paired Student's t-test). Furthermore, in high-grade tumors with gadolinium enhancement, the tumor core intensity was found to be much higher in comparison to the intensity in regions assumed to represent tumor periphery, and also to the CNAWM. For low-grade tumors (N = 5), the image intensity was also found to be significantly higher in the tumor region in comparison to the CNAWM ($p = 0.034$, paired Student's t-test), but

this increase was not as significant as for high-grade tumors. Finally, when comparing signal intensities obtained in tumors of high and low-grade, high-grade tumors appeared to have a significant increase in signal in comparison to low-grade tumors ($p = 0.02$, Student's t-test).

Below, some illustrative cases are shown.

Patient 2:

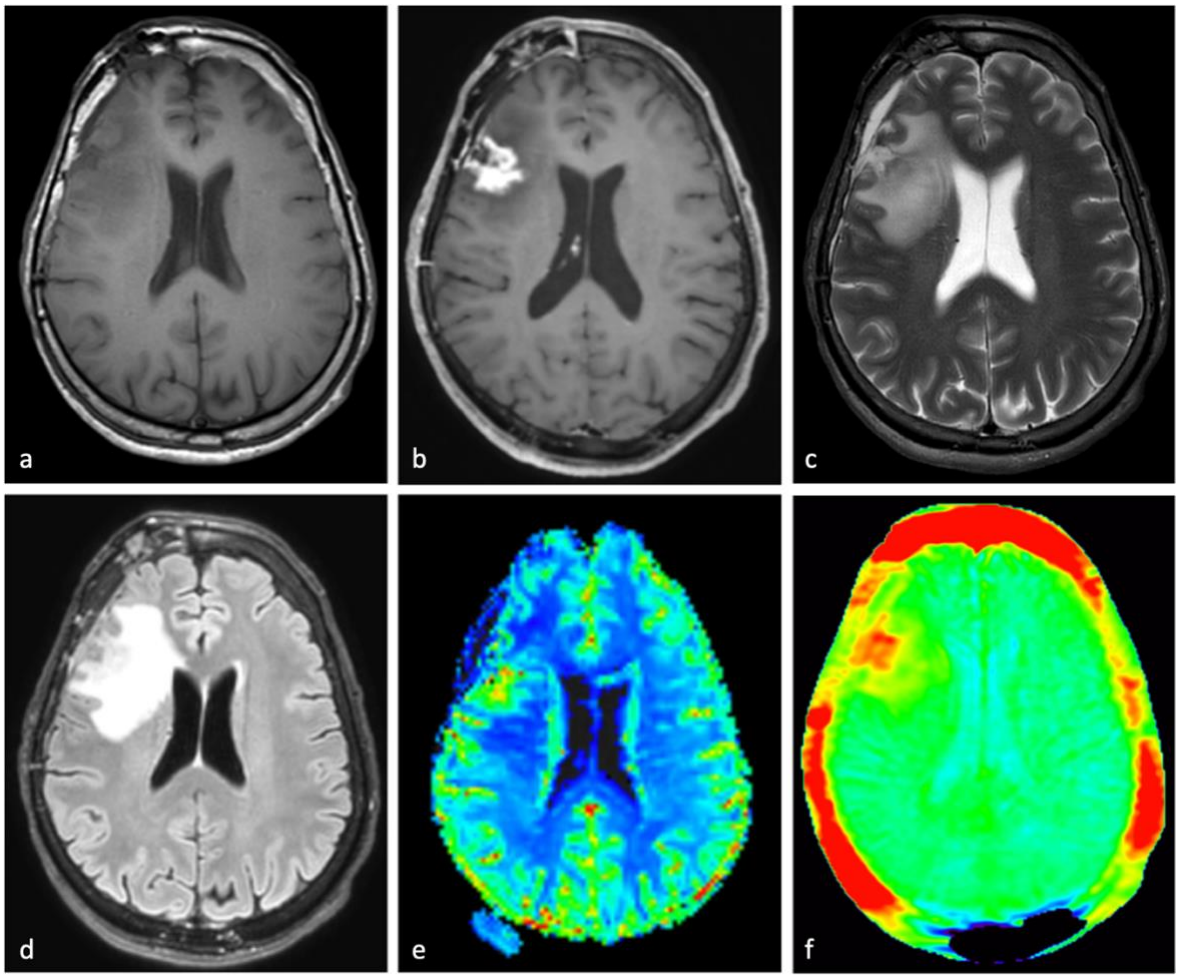

Fig. 1. MR images of patient 2, who has a glioblastoma IDH-wildtype (WHO grade 4). **a.** T1-w image. **b.** Gd-T1w image. **c.** T2-w image. **d.** T2-FLAIR image. **e.** DSC perfusion study. **f.** APT-w image.

Fig. 1 shows data for patient 2. The T1-w, T2-w, and T2-FLAIR images (Fig. 1a, c and d) show a large lesion in the right frontal lobe of heterogenous density with hypodense, isodense and discretely hyperdense regions. The large hyperintense region on T2-FLAIR (Fig. 1d) is considered to represent the full extent of the tumor while the Gd-T1w image (Fig. 1b) shows areas within the tumor where the blood brain barrier has been disrupted, considered the tumor core. Although these two areas can be clearly identified, the distinction between them is sometimes not that clear. Fig. 1f, shows the APT-w image of the same patient, where a bright red area can be seen on

the right frontal lobe. This is the region with the highest APT signal intensity in this patient´s brain (3.36 ± 0.53), clearly increased in comparison to the normal appearing white matter (NAWM), and to the surrounding tumor (seen in yellow), which only appears to have a mild increase in signal intensity (1.15 ± 0.31) in comparison to the NAWM (0.51 ± 0.20). The bright red area appears to be correlated with the most solid aspects of the tumor. It is much smaller than the abnormal area on T2-w, T1-w and T2-FLAIR images, and although it appears to be related to the gadolinium enhancing region on the Gd-T1w image, the two areas do not completely overlap. Furthermore, regions with lower APT signal intensity, but still increased in comparison to NAWM, appear to be related to the periphery of the tumor.

The histopathological study revealed a glioblastoma IDH-wildtype (WHO grade 4).

Patient 3:

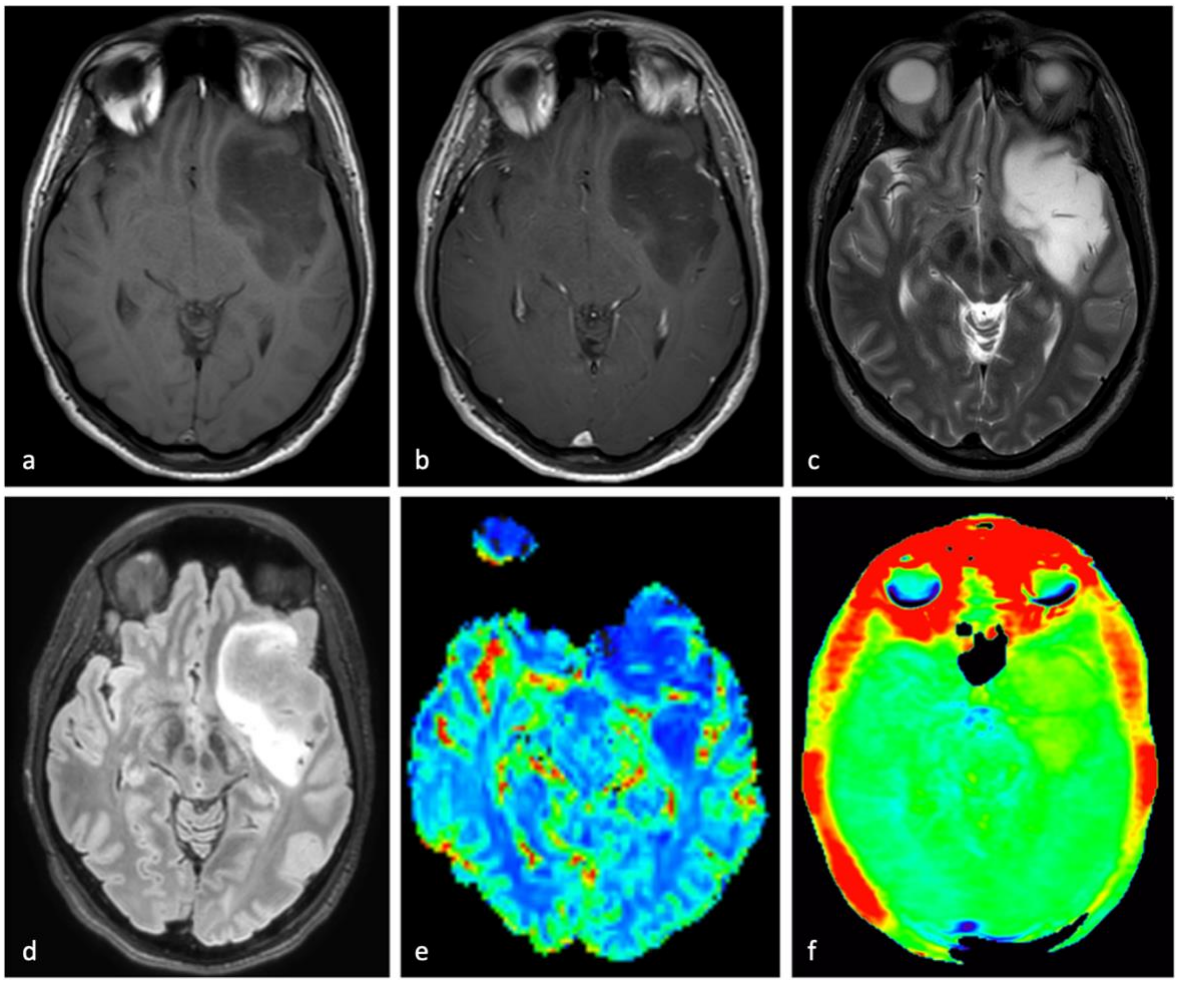

Fig. 2. MR images of patient 3, with an astrocytoma IDH-mutated (WHO grade 3). **a.** T1-w image. **b.** Gd-T1w image. **c.** T2-w image. **d.** T2-FLAIR image. **e.** DSC perfusion study. **f.** APT-w image.

Fig. 2 shows MR images of patient 3. T1-w, T2-w and T2-FLAIR images (Fig. 1a, c and d) show a large lesion located in the left frontal and temporal lobes homogeneously hyperintense on T2-w, hypointense on T1-w, and partially attenuated on T2-FLAIR suggesting the presence of T2/FLAIR mismatch sign, considered a highly specific radiogenomic signature for astrocytomas, as opposed to other low-grade gliomas.[64] This tumor does not show any contrast enhancement on Gd-T1w (Fig. 2b) and has no signs of greater aggressiveness or malignancy such as heterogenous areas of contrast enhancement or an increased cerebral blood volume (CBV) in the perfusion study (Fig. 2e). However, the APT-w image (Fig. 2f) shows a yellow area of discrete and diffuse elevation in signal (2.21 ± 0.13), in comparison to NAWM (0.34 ± 0.22). This region is comparable in size to that on the T2-w, T1-w and T2-FLAIR images, but they do not completely overlap.

The histopathological study revealed a WHO grade 3 IDH-mutated astrocytoma.

Patient 5:

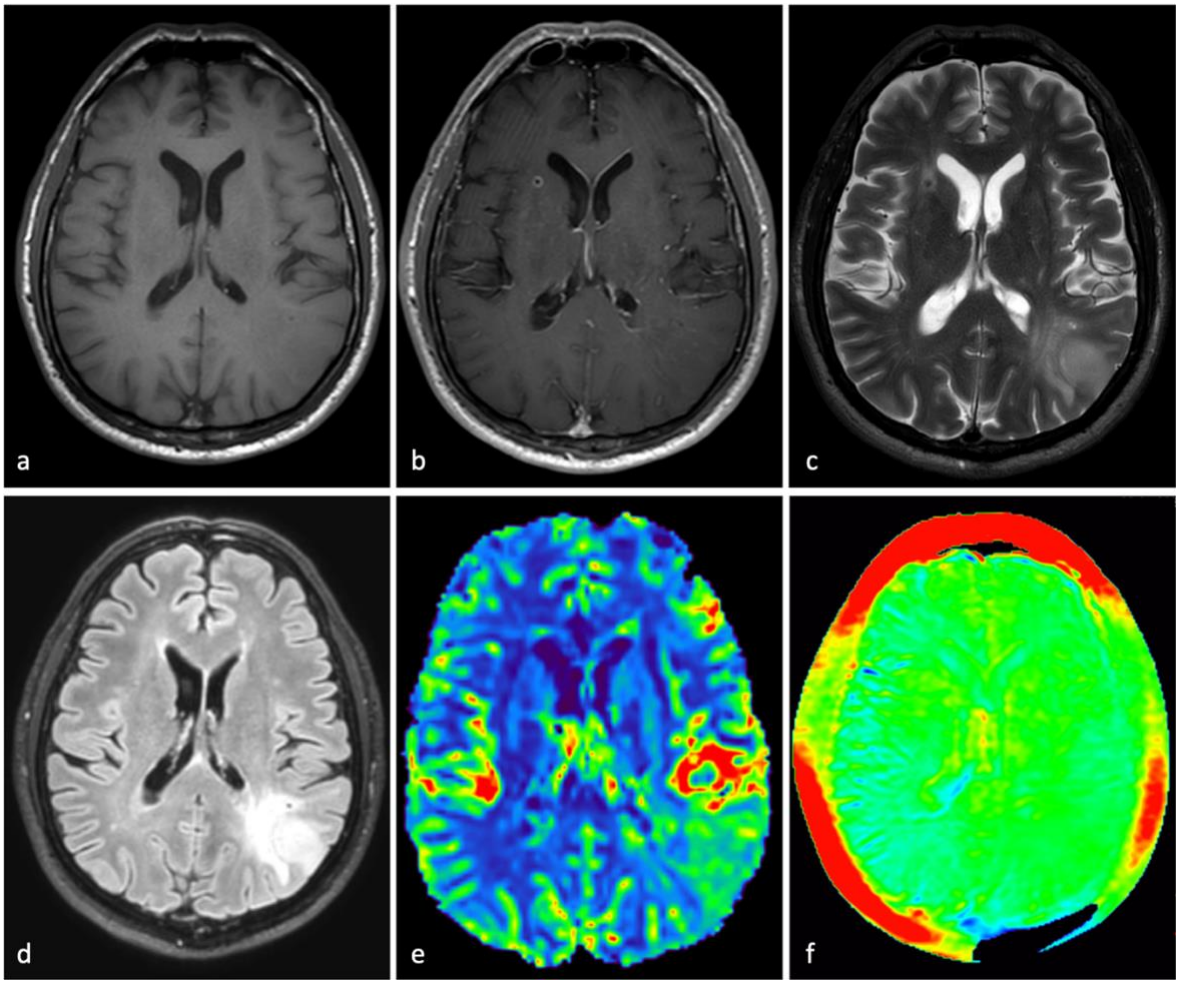

Fig. 3. MR images of patient 5, with a low-grade glioma. **a.** T1-w image. **b.** Gd-T1w image. **c.** T2-w image. **d.** T2-FLAIR image. **e.** DSC perfusion study. **f.** APT-w image.

Fig. 3 shows MR images of patient 5. A lesion can be seen on the left parietal and occipital lobes, showing expansive and infiltrative behaviour, with heterogenous signal, in general hyperintense in T2-w (Fig. 3c) and T2-FLAIR (Fig. 3d), and no enhancement after contrast injection (Fig. 3b). Also, a small nodular lesion in the right insular area can be seen, which represents a calcified granuloma. Interestingly, T1-w, T2-w and T2-FLAIR images all highlight the tumor, and the perfusion study shows an increase in CBV (Fig. 3e), while no obvious lesion or signal enhancement can be found in this region on either APT-w (Figure 3) or Gd-T1w images. However, signal intensity measured in the area of the tumor was found to be slightly increased (1.29 ± 0.21) in comparison to NAWM (0.18 ± 0.18).

At the time of this analysis, the patient had not yet undergone a tumor biopsy. According to findings in conventional MRI sequences, we presume this might be a low-grade tumor, also suggested by the patient's long history of adult epilepsy, which began four years before the diagnosis. Although the elevation in CBV previously described is a characteristic usually seen in more aggressive tumors, it may also be present in some low-grade tumors, such as oligodendrogliomas.

Discussion

Gliomas are a heterogenous group of primary central nervous system (CNS) tumors, which constitute the most common type of malignant primary CNS tumor in adults. They originate from glial progenitor cells, forming highly infiltrative lesions consisting of cores of solid tumor, sometimes mixed with necrosis, surrounded by regions of edematous brain that are often infiltrated by tumor cells.[65] As previously mentioned, although MRI is the standard of care for the evaluation of these tumors, it sill poses several limitations, especially regarding its ability to delineate solid tumor from peritumoral vasogenic edema, and to predict tumor histopathologic grade. An example of this is the hyperintensity observed on a T2-w image of a glial brain tumor, which may be either due to tumor infiltration or peritumoral vasogenic edema.[12,13,14] At the same time, a Gd-T1w image only reveals focal areas of malignant tissue if the blood-brain barrier is disrupted.[15] In regard to tumor grade prediction, gadolinium enhancement in MRI is not always specific for estimating tumor grade, as some low-grade gliomas occasionally enhance[55] and some high-grade gliomas show no enhancement[56]. Currently, perfusion studies are considered the best method of estimating histopathologic grade, by using the rCBV. High-grade gliomas have regions of higher rCBV in comparison to low-grade gliomas. But again, even this rule has exceptions, which include the pilocytic astrocytoma and oligodendroglioma, which can show foci of high rCBV that does not relate to tumor grade.[44]

During brain resection surgery attempts are made to limit the resection of brain tissue affected by edema, as these areas may be able to recover normal function.[1] Consequently, there is an urgent need for a new imaging technique, that is able to make a more accurate distinction between potentially recoverable brain tissue, and malignant tissue that must be removed. APT imaging is a new MRI technique which may provide more accurate visual and quantitative information about tumor grade and tumor margins, distinct from that provided by conventional MRI sequences.[11]

Data from Table I shows a comparison of APT signal intensities between tumors of different histopathologic grades, and between different regions of the same tumor. Our results show a general increase in APT signal intensity in malignant tissues, in comparison to NAWM, which is much more accentuated in high-grade tumors, as they also show a significantly higher APT intensity in comparison to low-grade tumors. In tumors where there is a distinction between core and periphery (gadolinium enhancing tumors), the APT signal obtained from the tumor core has also been shown to be significantly higher than the one obtained from the periphery of the tumor.

Regarding APT sequences of WHO grade 4 glioblastomas, which typically show contrast enhancement, these tumors are normally represented by a bright red area (corresponding to the highest APT signal intensity), which is not typically seen in patients with WHO grade 3 non-enhancing brain tumors. These non-enhancing tumors were found to have a slightly lower APT signal intensity in comparison to gadolinium enhancing WHO grade 4 tumors, but still significantly higher than that of NAWM. In these cases, APT images usually show a discrete and diffuse increase in signal, represented by a light yellow area, somewhat related to the area of hyperintensity seen on T2-FLAIR images. On the other hand, low-grade brain tumors (which typically show no gadolinium-enhancement) show no obvious hyperintense areas on APT-w color maps, but their measured signal intensity is slightly increased.

Our findings suggest that APT-w imaging might be a useful technique in the identification of brain tumors, and in the distinction between high and low-grade astrocytomas, possibly even in more detail, differentiating WHO grade 3 from WHO grade 4 tumors. From the four high-grade brain tumors we studied, only one case, patient 4, had an APT signal intensity closer to that of a low-grade brain tumor. We suspect this might be due to the fact that this patient had already undergone a brain biopsy, which aims to resect the most aggressive region of the lesion in order to obtain a final diagnosis and histopathologic grade. As a result, the lesion we observed on our study could have been only the remainder of the tumor, probably of a lower, less-aggressive grade.

We also found that in high-grade tumors, the hyperintense regions on APT-w images are usually larger than the areas of contrast enhancement on Gd-T1w images (in tumors that enhance), but smaller than the abnormal areas designated as tumor on T1-w, T2-w and T2-FLAIR images. Furthermore, on enhancing tumors, the bright red areas with the highest APT signal are probably related to the most solid regions of the tumor (gadolinium enhancing areas), although the two of them do not usually completely overlap. These red areas are usually found inside a region of lower APT signal (yellow regions) in comparison to the tumor core, but higher than that of NAWM, which are assumed to represent tumor periphery. These areas probably correspond to areas of lower grade inside a high-grade tumor, as their APT signal intensity is similar to that of lower-grade tumors.

These findings, once confirmed by targeted biopsies of different regions assumed to represent tumor core, tumor periphery and edema, may prove how APT-w imaging has the capability of distinguishing tumor boundaries more accurately than the MRI sequences currently in use, which

might be a great advantage when guiding tumor resection surgery. Furthermore, this technique might have another very important use related to determining histopathologic grade. It may be able to identify the areas of highest grade within a brain tumor, essentially identifying which areas should be biopsied in order to obtain a more accurate histopathologic grade.

Conclusion

This work has definitely established APT imaging as a feasible tool for the pre-surgical characterization of brain tumors in routine clinical practice at ULSSA.

Although this data was collected from a small sample, APT imaging has been shown to be an additional useful tool for the characterization of brain tumors, potentially delineating tumor core from peritumoral edema more accurately than gadolinium-based imaging alone. Such data, when validated by targeted biopsies used to associate histopathology with different APT intensities, could verify the viability of this imaging technique for the planning of maximal tumor resections. It is possible that surgery guided by areas of APT hyperintensity may reduce tumor recurrence, which, in 80% of cases, occurs in resection margins.[37-43]

Furthermore, the highest APT signal intensity has been found to be correlated to tumor aggressiveness and histopathologic grade. This technique may be able to distinguish high from low-grade brain tumors with more accuracy than other techniques currently in use, even showing capability to distinguish WHO grade 3 from WHO grade 4 tumors. APT-w imaging is also able to identify areas of higher malignancy within a tumor and consequently, determine precisely which areas should be biopsied in order to obtain a more accurate histopathologic grade.

References

1. Verburg, N., & De Witt Hamer, P. C. (2020). State-of-the-art imaging for glioma surgery. *Neurosurgical Review*, *44*(3), 1331–1343.
2. Oh, J., Cha, S., Aiken, A. H., Han, E. T., Crane, J. C., Stainsby, J. A., Wright, G. A., Dillon, W. P., & Nelson, S. J. (2005). Quantitative apparent diffusion coefficients and T2 relaxation times in characterizing contrast enhancing brain tumors and regions of peritumoral edema. *Journal of Magnetic Resonance Imaging*, *21*(6), 701–708.
3. Lev, M. H., & Hochberg, F. (1998). Perfusion Magnetic Resonance Imaging to Assess Brain Tumor Responses to New Therapies. *Cancer Control*, *5*(2), 115–123.
4. Akella, N. S., Twieg, D. B., Mikkelsen, T., Hochberg, F. H., Grossman, S., Cloud, G. A., & Nabors, L. B. (2004). Assessment of brain tumor angiogenesis inhibitors using perfusion magnetic resonance imaging: Quality and analysis results of a phase I trial. *Journal of Magnetic Resonance Imaging*, *20*(6), 913–922.
5. Gauvain, K. M., McKinstry, R. C., Mukherjee, P., Perry, A., Neil, J. J., Kaufman, B. A., & Hayashi, R. J. (2001). Evaluating Pediatric Brain Tumor Cellularity with Diffusion-Tensor Imaging. *American Journal of Roentgenology*, *177*(2), 449–454.
6. Mori, S., Frederiksen, K., Van Zijl, P. C. M., Stieltjes, B., Kraut, M. A., Solaiyappan, M., & Pomper, M. G. (2002). Brain white matter anatomy of tumor patients evaluated with diffusion tensor imaging. *Annals of Neurology*, *51*(3), 377–380.
7. Ulmer, J. L., Salvan, C. V., Mueller, W. M., Krouwer, H. G., Stroe, G. O., Aralasmak, A., & Prost, R. W. (2004). The Role of Diffusion Tensor Imaging in Establishing the Proximity of Tumor Borders to Functional Brain Systems: Implications for Preoperative Risk Assessments and Postoperative Outcomes. *Technology in Cancer Research & Treatment*, *3*(6), 567–576.
8. Alger, J. R., Frank, J. A., Bizzi, A., Fulham, M. J., DeSouza, B. X., Duhaney, M. O., Inscoe, S. W., Black, J. L., Van Zijl, P. C., & Moonen, C. T. (1990). Metabolism of human gliomas: assessment with H-1 MR spectroscopy and F-18 fluorodeoxyglucose PET. *Radiology*, *177*(3), 633–641.
9. McKnight, T. R., Von Dem Bussche, M. H., Vigneron, D. B., Lu, Y., Berger, M. S., McDermott, M. W., Dillon, W. P., Graves, E. E., Pirzkall, A., & Nelson, S. J. (2002). Histopathological validation of a three-dimensional magnetic resonance spectroscopy index as a predictor of tumor presence. *Journal of Neurosurgery*, *97*(4), 794–802.
10. *Multivoxel magnetic resonance spectroscopy of brain tumors*. (2003, May 1). PubMed.
11. Zhou, J., Heo, H., Knutsson, L., Van Zijl, P. C., & Jiang, S. (2019). APT-weighted MRI: Techniques, current neuro applications, and challenging issues. *Journal of Magnetic Resonance Imaging*, *50*(2), 347–364.
12. Graif, M., Bydder, G. M., Steiner, R. E., Niendorf, P., Thomas, D. G., & Young, I. R. (1985, November 1). *Contrast-enhanced MR imaging of malignant brain tumors.* American Journal of Neuroradiology.
13. Jones, C. K., Schlosser, M. J., Van Zijl, P. C., Pomper, M. G., Golay, X., & Zhou, J. (2006). Amide proton transfer imaging of human brain tumors at 3T. *Magnetic Resonance in Medicine*, *56*(3), 585–592.
14. *Diffusion-weighted MR imaging of intracerebral masses: comparison with conventional MR imaging and histologic findings*. (2001, May 1). PubMed.
15. Burger, P. C., Heinz, E. R., Shibata, T., & Kleihues, P. (1988). Topographic anatomy and CT correlations in the untreated glioblastoma multiforme. *Journal of Neurosurgery*, *68*(5), 698–704.
16. Eidel, O., Burth, S., Neumann, J. O., Kieslich, P. J., Sahm, F., Jungk, C., Kickingereder, P., Bickelhaupt, S., Mundiyanapurath, S., Bäumer, P., Wick, W., Schlemmer, H. P., Kiening, K., Unterberg, A., Bendszus, M., & Radbruch, A. (2017). Tumor Infiltration in Enhancing and Non-Enhancing Parts of Glioblastoma: A Correlation with Histopathology. *PloS One*, *12*(1), e0169292.
17. Ward, K., Aletras, A., & Balaban, R. (2000). A New Class of Contrast Agents for MRI Based on Proton Chemical Exchange Dependent Saturation Transfer (CEST). *Journal of Magnetic Resonance*, *143*(1), 79–87.

18. Zhang, S., Merritt, M., Woessner, D. E., Lenkinski, R. E., & Sherry, A. D. (2003). PARACEST Agents: Modulating MRI Contrast via Water Proton Exchange. *Accounts of Chemical Research*, *36*(10), 783–790.
19. Zhou, J., & Van Zijl, P. C. (2006). Chemical exchange saturation transfer imaging and spectroscopy. *Progress in Nuclear Magnetic Resonance Spectroscopy*, *48*(2–3), 109–136.
20. Sherry, A. D., & Woods, M. (2008). Chemical Exchange Saturation Transfer Contrast Agents for Magnetic Resonance Imaging. *Annual Review of Biomedical Engineering*, *10*(1), 391–411.
21. Kogan, F., Hariharan, H., & Reddy, R. (2013). Chemical Exchange Saturation Transfer (CEST) Imaging: Description of Technique and Potential Clinical Applications. *Current Radiology Reports*, *1*(2), 102–114.
22. Vinogradov, E., Sherry, A. D., & Lenkinski, R. E. (2013). CEST: From basic principles to applications, challenges and opportunities. *Journal of Magnetic Resonance*, *229*, 155–172.
23. Van Zijl, P. C., Lam, W. W., Xu, J., Knutsson, L., & Stanisz, G. J. (2018). Magnetization Transfer Contrast and Chemical Exchange Saturation Transfer MRI. Features and analysis of the field-dependent saturation spectrum. *NeuroImage*, *168*, 222–241.
24. Jones, K. M., Pollard, A. C., & Pagel, M. D. (2017). Clinical applications of chemical exchange saturation transfer (CEST) MRI. *Journal of Magnetic Resonance Imaging*, *47*(1), 11–27.
25. Bai, Y., Lin, Y., Zhang, W., Kong, L., Wang, L., Zuo, P., Vallines, I., Schmitt, B., Tian, J., Song, X., Zhou, J., & Wang, M. (2016). Noninvasive amide proton transfer magnetic resonance imaging in evaluating the grading and cellularity of gliomas. *Oncotarget*, *8*(4), 5834–5842.
26. Knutsson, L., Xu, J., Ahlgren, A., & Van Zijl, P. C. (2018). CEST, ASL, and magnetization transfer contrast: How similar pulse sequences detect different phenomena. *Magnetic Resonance in Medicine*, *80*(4), 1320–1340.
27. Ven, K. V. D., & Keupp, J. (2018). *Amide Proton Transfer weighted imaging : Advancement in molecular tumor diagnosis*.
28. Van Zijl, P. C. M., & Yadav, N. N. (2011). Chemical exchange saturation transfer (CEST): What is in a name and what isn't? *Magnetic Resonance in Medicine*, *65*(4), 927–948.
29. Zhou, J., Lal, B., Wilson, D. A., Laterra, J., & Van Zijl, P. C. (2003). Amide proton transfer (APT) contrast for imaging of brain tumors. *Magnetic Resonance in Medicine*, *50*(6), 1120–1126.
30. Zhou, J., Payen, J. F., Wilson, D. A., Traystman, R. J., & Van Zijl, P. C. M. (2003b). Using the amide proton signals of intracellular proteins and peptides to detect pH effects in MRI. *Nature Medicine*, *9*(8), 1085–1090.
31. Goffeney, N., Bulte, J. W. M., Duyn, J., Bryant, L. H., & Van Zijl, P. C. M. (2001). Sensitive NMR Detection of Cationic-Polymer-Based Gene Delivery Systems Using Saturation Transfer via Proton Exchange. *Journal of the American Chemical Society*, *123*(35), 8628–8629.
32. McMahon, M. T., Gilad, A. A., Zhou, J., Sun, P. Z., Bulte, J. W. M., & Van Zijl, P. C. M. (2006). Quantifying exchange rates in chemical exchange saturation transfer agents using the saturation time and saturation power dependencies of the magnetization transfer effect on the magnetic resonance imaging signal (QUEST and QUESP): Ph calibration for poly-L-lysine and a starburst dendrimer. *Magnetic Resonance in Medicine*, *55*(4), 836–847.
33. Gilad, A. A., McMahon, M. T., Walczak, P., Winnard, P. T., Raman, V., Van Laarhoven, H. W. M., Skoglund, C. M., Bulte, J. W. M., & Van Zijl, P. C. M. (2007). Artificial reporter gene providing MRI contrast based on proton exchange. *Nature Biotechnology*, *25*(2), 217–219.
34. Sun, P. Z., Zhou, J., Sun, W., Huang, J., & Van Zijl, P. C. (2006). Detection of the Ischemic Penumbra Using pH-Weighted MRI. *Journal of Cerebral Blood Flow and Metabolism*, *27*(6), 1129–1136.
35. Jokivarsi, K. T., Gröhn, H. I., Gröhn, O. H., & Kauppinen, R. A. (2007). Proton transfer ratio, lactate, and intracellular pH in acute cerebral ischemia. *Magnetic Resonance in Medicine*, *57*(4), 647–653.
36. Howe, F., Barton, S., Cudlip, S., Stubbs, M., Saunders, D., Murphy, M., Wilkins, P., Opstad, K., Doyle, V., McLean, M., Bell, B., & Griffiths, J. (2003). Metabolic profiles of human brain tumors using quantitative in vivo 1H magnetic resonance spectroscopy. *Magnetic Resonance in Medicine*, *49*(2), 223–232.

37. Zhou, J., Blakeley, J. O., Hua, J., Kim, M., Laterra, J., Pomper, M. G., & Van Zijl, P. C. (2008). Practical data acquisition method for human brain tumor amide proton transfer (APT) imaging. *Magnetic Resonance in Medicine*, *60*(4), 842–849.
38. Wen, Z., Hu, S., Huang, F., Wang, X., Guo, L., Quan, X., Wang, S., & Zhou, J. (2010). MR imaging of high-grade brain tumors using endogenous protein and peptide-based contrast. *NeuroImage*, *51*(2), 616–622.
39. Jiang, S., Yu, H., Wang, X., Lu, S., Li, Y., Feng, L., Zhang, Y., Heo, H. Y., Lee, D. H., Zhou, J., & Wen, Z. (2015). Molecular MRI differentiation between primary central nervous system lymphomas and high-grade gliomas using endogenous protein-based amide proton transfer MR imaging at 3 Tesla. *European Radiology*, *26*(1), 64–71.
40. *Yu H, Lou H, Zou T, et al. Applying protein-based amide proton transfer MR imaging to distinguish solitary brain metastases from glioblastoma. Eur Radiol 2017;27:4516–24. [PubMed: 28534162] - Google Search*. (n.d.).
41. Sakata, A., Fushimi, Y., Okada, T., Arakawa, Y., Kunieda, T., Minamiguchi, S., Kido, A., Sakashita, N., Miyamoto, S., & Togashi, K. (2017). Diagnostic performance between contrast enhancement, proton MR spectroscopy, and amide proton transfer imaging in patients with brain tumors. *Journal of Magnetic Resonance Imaging*, *46*(3), 732–739.
42. Joo, B., Han, K., Choi, Y. S., Lee, S. K., Ahn, S. S., Chang, J. H., Kang, S. G., Kim, S. H., & Zhou, J. (2017). Amide proton transfer imaging for differentiation of benign and atypical meningiomas. *European Radiology*, *28*(1), 331–339.
43. Sun, H., Xin, J., Zhou, J., Lu, Z., & Guo, Q. (2017). Applying Amide Proton Transfer MR Imaging to Hybrid Brain PET/MR: Concordance with Gadolinium Enhancement and Added Value to [18F]FDG PET. *Molecular Imaging and Biology*, *20*(3), 473–481.
44. Sled, J. G., & Pike, G. B. (2001). Quantitative imaging of magnetization transfer exchange and relaxation properties in vivo using MRI. *Magnetic Resonance in Medicine*, *46*(5), 923–931.
45. Jiang, S., Eberhart, C. G., Zhang, Y., Heo, H. Y., Wen, Z., Blair, L., Qin, H., Lim, M., Quinones-Hinojosa, A., Weingart, J. D., Barker, P. B., Pomper, M. G., Laterra, J., Van Zijl, P. C., Blakeley, J. O., & Zhou, J. (2017). Amide proton transfer-weighted magnetic resonance image-guided stereotactic biopsy in patients with newly diagnosed gliomas. *European Journal of Cancer*, *83*, 9–18.
46. Zhou, J., Zhu, H., Lim, M., Blair, L., Quinones-Hinojosa, A., Messina, S. A., Eberhart, C. G., Pomper, M. G., Laterra, J., Barker, P. B., Van Zijl, P. C., & Blakeley, J. O. (2013). Three-dimensional amide proton transfer MR imaging of gliomas: Initial experience and comparison with gadolinium enhancement. *Journal of Magnetic Resonance Imaging*, *38*(5), 1119–1128.
47. Togao, O., Yoshiura, T., Keupp, J., Hiwatashi, A., Yamashita, K., Kikuchi, K., Suzuki, Y., Suzuki, S. O., Iwaki, T., Hata, N., Mizoguchi, M., Yoshimoto, K., Sagiyama, K., Takahashi, M., & Honda, H. (2013). Amide proton transfer imaging of adult diffuse gliomas: correlation with histopathological grades. *Neuro-oncology*, *16*(3), 441–448.
48. Sakata, A., Okada, T., Yamamoto, A., Kanagaki, M., Fushimi, Y., Okada, T., Dodo, T., Arakawa, Y., Schmitt, B., Miyamoto, S., & Togashi, K. (2015). Grading glial tumors with amide proton transfer MR imaging: different analytical approaches. *Journal of Neuro-oncology*, *122*(2), 339–348.
49. Togao, O., Hiwatashi, A., Yamashita, K., Kikuchi, K., Keupp, J., Yoshimoto, K., Kuga, D., Yoneyama, M., Suzuki, S. O., Iwaki, T., Takahashi, M., Iihara, K., & Honda, H. (2016). Grading diffuse gliomas without intense contrast enhancement by amide proton transfer MR imaging: comparisons with diffusion- and perfusion-weighted imaging. *European Radiology*, *27*(2), 578–588.
50. Su, C., Liu, C., Zhao, L., Jiang, J., Zhang, J., Li, S., Zhu, W., & Wang, J. (2017). Amide Proton Transfer Imaging Allows Detection of Glioma Grades and Tumor Proliferation: Comparison with Ki-67 Expression and Proton MR Spectroscopy Imaging. *American Journal of Neuroradiology*, *38*(9), 1702–1709.
51. Choi, Y. S., Ahn, S. S., Lee, S. K., Chang, J. H., Kang, S. G., Kim, S. H., & Zhou, J. (2017). Amide proton transfer imaging to discriminate between low- and high-grade gliomas: added value to apparent diffusion coefficient and relative cerebral blood volume. *European Radiology*, *27*(8), 3181–3189.

52. Zou, T., Yu, H., Jiang, C., Wang, X., Jiang, S., Rui, Q., Mei, Y., Zhou, J., & Wen, Z. (2017). Differentiating the histologic grades of gliomas preoperatively using amide proton transfer-weighted (APTW) and intravoxel incoherent motion MRI. *NMR in Biomedicine*, *31*(1).
53. *Zhang J, Zhu W, Tain R, Zhou XJ, Cai K. Improved differentiation of low-grade and high-grade gliomas and detection of tumor proliferation using APT contrast fitted from Z-spectrum. Mol Imaging Biol 2018;20:623–31. [PubMed: 29313159] - Google Search*. (n.d.).
54. Park, J. E., Kim, H. S., Park, K. J., Kim, S. J., Kim, J. H., & Smith, S. A. (2016). Pre- and Posttreatment Glioma: Comparison of Amide Proton Transfer Imaging with MR Spectroscopy for Biomarkers of Tumor Proliferation. *Radiology*, *278*(2), 514–523.
55. Knopp, E. A., Cha, S., Johnson, G., Mazumdar, A., Golfinos, J. G., Zagzag, D., Miller, D. C., Kelly, P. J., & Kricheff, I. I. (1999). Glial Neoplasms: Dynamic Contrast-enhanced T2*-weighted MR Imaging. *Radiology*, *211*(3), 791–798.
56. Scott, J. N., Brasher, P. M., Sevick, R. J., Rewcastle, N. B., & Forsyth, P. A. (2002). How often are nonenhancing supratentorial gliomas malignant? A population study. *Neurology*, *59*(6), 947–949.
57. Wen, P. Y., Macdonald, D. R., Reardon, D. A., Cloughesy, T. F., Sorensen, A. G., Galanis, E., DeGroot, J., Wick, W., Gilbert, M. R., Lassman, A. B., Tsien, C., Mikkelsen, T., Wong, E. T., Chamberlain, M. C., Stupp, R., Lamborn, K. R., Vogelbaum, M. A., Van Den Bent, M. J., & Chang, S. M. (2010). Updated Response Assessment Criteria for High-Grade Gliomas: Response Assessment in Neuro-Oncology Working Group. *Journal of Clinical Oncology*, *28*(11), 1963–1972.
58. Zhou, J., Tryggestad, E., Wen, Z., Lal, B., Zhou, T., Grossman, R., Wang, S., Yan, K., Fu, D. X., Ford, E., Tyler, B., Blakeley, J., Laterra, J., & Van Zijl, P. C. M. (2010). Differentiation between glioma and radiation necrosis using molecular magnetic resonance imaging of endogenous proteins and peptides. *Nature Medicine*, *17*(1), 130–134.
59. Ma, B., Blakeley, J. O., Hong, X., Zhang, H., Jiang, S., Blair, L., Zhang, Y., Heo, H., Zhang, M., Van Zijl, P. C. M., & Zhou, J. (2016). Applying amide proton transfer-weighted MRI to distinguish pseudoprogression from true progression in malignant gliomas. *Journal of Magnetic Resonance Imaging*, *44*(2), 456–462.
60. Wang, S., Tryggestad, E., Zhou, T., Armour, M., Wen, Z., Fu, D. X., Ford, E., Van Zijl, P. C., & Zhou, J. (2012). Assessment of MRI Parameters as Imaging Biomarkers for Radiation Necrosis in the Rat Brain. *International Journal of Radiation Oncology, Biology, Physics*, *83*(3), e431–e436.
61. Hong, X., Liu, L., Wang, M., Ding, K., Fan, Y., Ma, B., Lal, B., Tyler, B., Mangraviti, A., Wang, S., Wong, J., Laterra, J., & Zhou, J. (2013). Quantitative multiparametric MRI assessment of glioma response to radiotherapy in a rat model. *Neuro-oncology*, *16*(6), 856–867.
62. Sagiyama, K., Mashimo, T., Togao, O., Vemireddy, V., Hatanpaa, K. J., Maher, E. A., Mickey, B. E., Pan, E., Sherry, A. D., Bachoo, R. M., & Takahashi, M. (2014). In vivo chemical exchange saturation transfer imaging allows early detection of a therapeutic response in glioblastoma. *Proceedings of the National Academy of Sciences of the United States of America*, *111*(12), 4542–4547.
63. Hectors, S. J., Jacobs, I., Strijkers, G. J., & Nicolay, K. (2013). Amide proton transfer imaging of high intensity focused ultrasound-treated tumor tissue. Magnetic Resonance in Medicine, 72(4), 1113–1122.
64. Pinto, C., Noronha, C., Taipa, R., & Ramos, C. (2022). T2-FLAIR mismatch sign: a roadmap of pearls and pitfalls. ˜the British Journal of Radiology/British Journal of Radiology, 95(1129).
65. Sanai, N., Alvarez-Buylla, A., & Berger, M. S. (2005). Neural Stem Cells and the Origin of Gliomas. New England Journal of Medicine/˜the New England Journal of Medicine, 353(8), 811–822.

INSTITUTO DE **CIÊNCIAS BIOMÉDICAS ABEL SALAZAR**